Photodiagnosis and Photodynamic Therapy 27 (2019) 280–287

Contents lists available at ScienceDirect

Photodiagnosis and Photodynamic Therapy

journal homepage: www.elsevier.com/locate/pdpdt

Antifungal effect of photodynamic therapy mediated by curcumin on *Candida albicans* biofilms *in vitro*

Jing Ma[1,a], Hang Shi[1,a], Hongying Sun[a,*], Jiyang Li[b], Yu Bai[a]

[a] Institution: Department of Stomatology, Huashan Hospital, Fudan University, No.12, Rd. Wulumuqi, Shanghai, China
[b] Institution: School of Pharmacy, Fudan University, No.826, Rd. Zhangheng, Shanghai, China

ARTICLE INFO

Keywords:
Candida albicans
Biofilm
Curcumin
Photodynamic therapy
Gene expression
Antimicrobial Photodynamic therapy

ABSTRACT

Background: : *Canida albicans* can cause opportunistic infections ranging from superficial mucous membrane lesions to life-threatening disease. The aim of this study is to investigate the antifungal effect of photodynamic therapy (PDT) mediated by curcumin (CUR) on *C. albicans* biofilms *in vitro*.

Methods: : One standard strain ATCC 90028 and two clinical isolates from HIV (CCA1) and oral lichen planus (CCA2) patients' oral cavities were used in this study. Biofilms were photosensitized with 60 μM CUR and irradiated by light emitting diode (LED) under the wavelength of 455 nm and energy densities of 2.64, 5.28, 7.92, 10.56, 13.2 J/cm^2. Then the antifungal effects of CUR-PDT were evaluated by XTT reduction assay and confocal light scanning microscopy (CLSM) observations. The effects of CUR-PDT on the expression levels of hypha-specific and biofilm-related genes including EFG1, UME6, HGC1 and ECE1 were assessed by quantitative Real-time PCR (qRT-PCR) method.

Results: : The inhibition rates after CUR-PDT in three biofilms(ATCC 90028, CCA1, CCA2)were 90.87%, 66.44% and 86.74% respectively ($p < 0.05$). Relative gene expression levels of EFG1, UME6, HGC1 and ECE1 were all downregulated after CUR-PDT, with fold-decrease of 6.865, 3.382, 2.167 and 6.887 in ATCC 90028, 2.466, 2.146, 1.627 and 3.102 in CCA1, and 5.406, 2.347, 2.073and 3.711 in CCA2 ($p < 0.05$).

Conclusions: : Curcumin-mediated PDT could effectively inactivate*Candida albicans* biofilms *in vitro*. Expression of genes involved in biofilms formation were downregulated after CUR-PDT.

1. Introduction

The oral cavity is colonized by a complex range of microorganisms. *C. albicans* is one of most virulent pathogenic fungus that inhabits half of human oral cavities [1]. Under certain circumstances, especially in immunocompromised host populations like HIV/AIDS patients, *C. albicans* can cause opportunistic infections ranging from superficial mucous membrane lesions to life-threatening diseases. In clinic, oral mucosal diseases including oral lichen planus (OLP) [2], oral leukoplakia [3], Sjogren syndrome [4], oral squamous cell carcinoma [5] etc, are often much harder to be cured if the lesions are infected by *C. albicans*.

One possible reason is that *C. albicans* forms surface-attached microbial communities known as biofilms [6]. Cells within biofilms are distinct from planktonic ones, which are more resistance to conventional antifungal drugs [7,8]. Therefore, the lack of effective antifungal agents and the emergence of drug-resistance *C. albicans* have driven researchers to seek alternative strategies, such as PDT [9,10].

PDT, a combination of a photosensitizer, light at specific wavelength, and oxygen is a selective and minimally invasive modality to treat a wide variety of disorders [11]. In dentistry, the antibacterial and antifungal properties of some photosensitizers have been used to achieve better results in root canal treatment, periodontal therapy and the eradication of candidiasis in prosthodontics [12–14]. Nevertheless, conventional photosensitizers such as methylene blue (MB) [15,16] and toluidine blue O (TBO) [13,17] showed limited effectiveness against *C. albicans* in oral mucosal infections, especially in biofilm forms.

CUR, a dye extracted from a plant *Curcuma longa*, is commonly used as a cooking spice and flavoring agent [18]. An increasing number of investigations have suggested that CUR exhibits great potential for its anti-inflammatory, anti-bacterial, anti-viral, and anti-tumor effects [19–23]. These functions can be enhanced by light, as it displays a high light absorption around 400–500 nm. Scientists further discovered that

* Corresponding author.
E-mail addresses: 16211220062@fudan.edu.cn (J. Ma), shihang1016@hotmail.com (H. Shi), sunhongying@fudan.edu.cn (H. Sun), lijiyang@fudan.edu.cn (J. Li), 313306489@qq.com (Y. Bai).
[1] Co-first authors.

https://doi.org/10.1016/j.pdpdt.2019.06.015
Received 23 April 2019; Received in revised form 11 June 2019; Accepted 20 June 2019
Available online 21 June 2019

CUR could be used as an effective photosensitizer for the yeast inactivation of *C. albicans* [24,25]. However, the mechanism is still unclear. To the best of our knowledge, there is no study elucidating the expression of biofilm-related genes in *C. albicans* after photodynamic inactivation mediated by CUR that has been reported. Here, for the first time, the action of CUR-PDT in gene expression of EFG1, UME6, HGC1 and ECE1 are studied.

In this study, we aim to investigate the antifungal effect of PDT mediated by CUR on biofilm-related *C. albicans in vitro*. Apart from standard strain, clinical isolated from HIV and OLP patients were analyzed as well for better evaluating the clinical relevance of *C. albicans*. Furthermore, the genetic changes of EFG1, UME6, HGC1 and ECE1 in *C. albicans* biofilms after CUR-PDT were investigated.

2. Materials and methods

2.1. Organism, reagent and growth conditions

Three specimens of *C. albicans* strains, including one standard strain ATCC 90028 (Department of Pharmacy, Fudan University, Shanghai, China), one clinical isolate (CCA1) from HIV-infected patient's oral cavity, and another clinical isolate (CCA2) from OLP patient's oral cavity were used in this study. Approval from the Institutional Review Board of Huashan hospital (HIRB) and written informed consents were obtained from both patients. Both clinical isolates were identified by CHROMagar™ technique. Fungal cells were maintained in Sabouraud dextrose agar (SDA) medium at -4 °C, and were reactivated by cultivation in the fresh SDA (28 °C, 48 h). Each single colony was inoculated into 30 mL YPD (Yeast Peptone Dextrose) liquid medium (1% w/v yeast extract, 2% w/v peptone, 2% w/v dextrose). The cultures were then incubated in an orbital shaker for 15 h (160 rpm) at 32 °C, centrifuged (3000 rpm, 10 min, 4 °C), and the harvested cells were washed twice with sterile phosphate buffered saline (PBS, pH 7.4). Then, cells were resuspended in RPMI-1640 (supplemented with L-glutamine, buffered with sodium bicarbonate) (Gibco, Grand Island, NY, USA), and adjusted to the final density of 1.0×10^6 cells/mL by counting cells with a hemacytometer.

2.2. Biofilms formation

Aliquots of 100 mL of the *C. albicans* suspensions were individually transferred to the separate wells of 96-well microtiter plates (100 μL /well), followed by incubation for 48 h at 37 °C. The biofilms were fixed with methanol for 20 min, and then stained with 0.01% crystal violet for 5 min. After that, the dye was rinsed thrice with PBS. The morphology of the biofilm formation process was captured under an inverted microscopy.

2.3. Photosensitizer and light source

The photosensitizer CUR (Sigma-Aldrich, Saint Louis, MO, USA) was prepared with 10% dimethyl sulfoxide (DMSO) to originate a stock solution, from which other solutions were diluted with physiological solution (0.85% NaCl) to the final concentrations of 20, 40, 60, 80 and 100 μM.

A light emitting diode (LED) device (Institute of Photoelectricity, Fudan University, Shanghai, China) was used to activate the CUR. The LED intensity of emitted light was 22.0 mW/cm^2 and the wavelength was 455 nm.

2.4. XTT reduction assays

XTT[2,3-bis(2-methoxy-4-nitro-5-sulfo-phenyl)-2H-tetrazolium-5-carboxanilide] (Sigma-Aldrich, St Louis, MO) was dissolved in PBS at a concentration of 1 mg/mL. Then the solution was sterilized using a 0.22 μm pore-size filter and stored at −80 °C. Menadione solution (Sigma; 0.4 mM) was prepared in acetone. Kinetics of *C.albicans* biofilms were measured over a series of time intervals (2, 6, 12, 24, 36, 48, 60 h). For each assay, the biofilms were washed with PBS to remove the planktonic cells. After that, 158 μL of PBS with 200 mM glucose, 40 μL of XTT and 2 μL of menadione solution were mixed, and 200 μL of the mixture were added to each well and incubated for 3 h in the dark at 37 °C. The intensity of the colorimetric reaction, reflecting its metabolic activity, was calculated by measuring the optical density at 492 nm (OD_{492}) using a spectrophotometer (BioTek Synergy 2, USA).

2.5. Photodynamic inactivation of C. albicans biofilms

Aliquots of 100 μL of CUR were added to each well of *C. albicans* biofilms in the dark for 20 min. Then, the residual CUR was removed and replaced by RPMI 1640. PDT experiments were carried out by illuminating CUR-treated *C. albicans* biofilms under a LED device.

Illumination was performed for 2, 4, 6, 8 and 10 min, resulting in a total fluence of 2.64, 5.28, 7.92, 10.56, 13.2 J/cm^2 respectively (C + L +). To determine whether CUR alone had any effect on cell viability, additional wells containing mature biofilms were exposed to CUR under identical conditions as described above, without LED light (C + L-). The effect of LED light alone was determined by exposing cells to light without being previously exposed to CUR (C-L+). Biofilms exposed to neither CUR nor LED light acted as control group (C-L-). After PDT, XTT reduction assay was used again to obtain the optical parameters of PDT in our study. The inhibition rate was calculated as follows: % inhibition rate = [OD_{492} (C-L-)-OD_{492} (C + L+)]/ OD_{492} (C-L-).

2.6. Confocal laser scanning microscopy (CLSM) observations

CLSM was performed to demonstrate the inhibitory effect of PDT on *C. albicans* biofilms. The LIVE/DEAD® FungalLight™ Yeast Viability Kit (Molecular Probes, Eugene, OR, USA) containing SYTO-9 and Propidium Iodide (PI) was used to probe live and dead cells.

Three specimens of *C. albicans* biofilms were prepared as described above and placed on 10-mm round coverslips. 400 μL of the fluorescent solution was added to each coverslip and incubated at room temperature for 15 min in the dark. Stained biofilms were flipped and placed on a glass-bottom and observed using a Zeiss CLSM (LSM 710, Zeiss, Germany). The maximum excitation/emission used for observation was 480/500 nm for SYTO9, and 490/635 nm for PI. For each sample, images from three randomly selected positions were acquired.

2.7. Quantitative real-time PCR (qRT-PCR) assays

Total RNA was extracted from biofilms with TRIzol reagent (Invitrogen) and resuspended in diethyl pyrocarbonate water. The concentration, purity and quality of the isolated RNA samples were determined using a Nano-Drop-One Spectrophotometer (Thermo Scientific, Waltham, MA, USA). First strand cDNA was synthesized from 3 μg of total RNA in a 60 μL reaction volume using the cDNA synthesis kit for quantitative real-time PCR (qRT-PCR) (TaKaRa Biotechnology, Dalian, China) in accordance with the manufacturer's instructions. Triplicate independent qRT-PCR assays were performed using the LightCycler® System (Roche Diagnostics GmbH, Mannheim, Germany). SYBR® Green (TaKaRa Biotechnology) was used to visualize and monitor the amplified product in real-time according to the manufacturer's protocol. Target genes EFG1, UME6, HGC1, and ECE1 were amplified accordingly. The expression levels of biofilm-associated genes were calculated relative to the calibration sample of endogenous control 16S rRNA to normalize the sample input.

2.8. Statistical analysis

All experiments were conducted in triplicate and repeated three times. The data were reported as the mean ± standard deviations. The

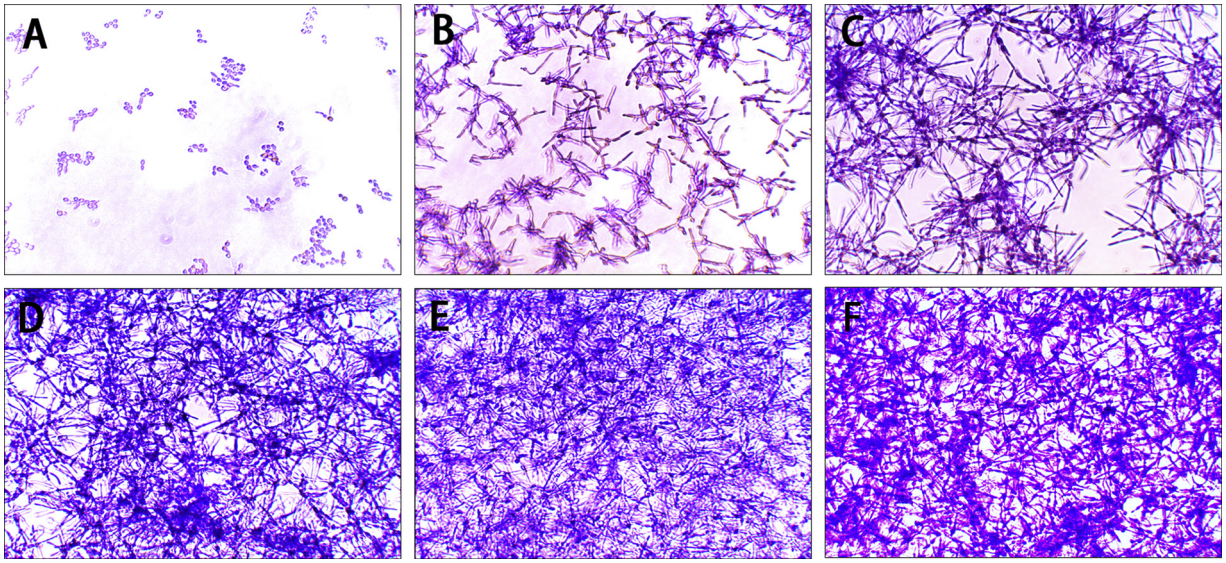

Fig. 1. Light microscopy images of *Candida albicans* biofilms formation over a 48-h period: ATCC 90028 2 h (A), ATCC 90028 12 h (B), ATCC 90028 24 h (C), ATCC 90028 48 h (D), CCA1 48 h (E), CCA2 48 h (F). Magnification, ×400.

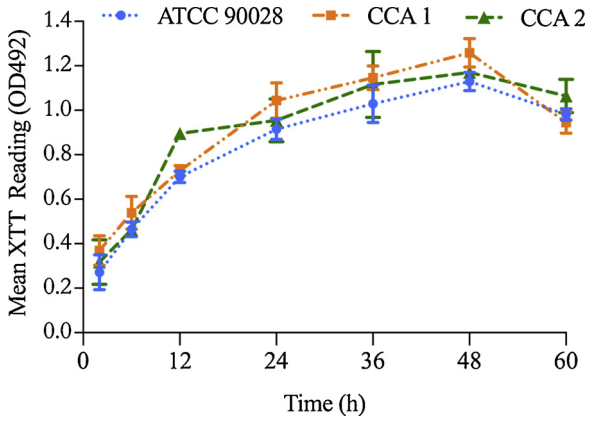

Fig. 2. Metabolic activity of *Candida albicans* biofilms estimated by XTT reduction assay. The data represent the mean ± standard deviation from two independent experiments performed in triplicate.

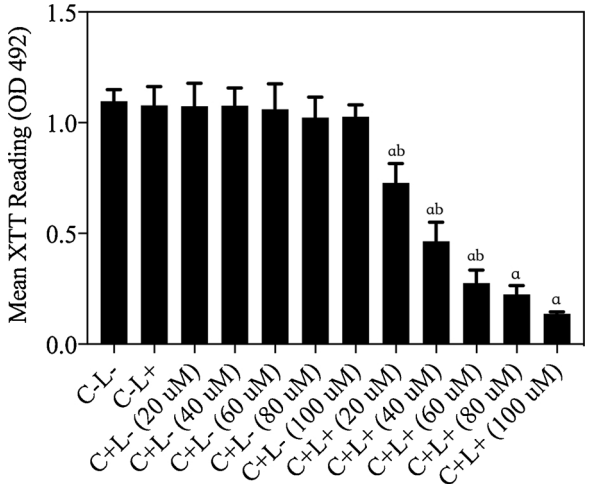

Fig. 3. Graphic representation of mean values and standard deviation of cell viabilities in ATCC 90028 *Candida albicans* biofilm under different curcumin concentrations.
[a], significant difference compared to control group (C-L-); [b], significant difference compared to the former group.

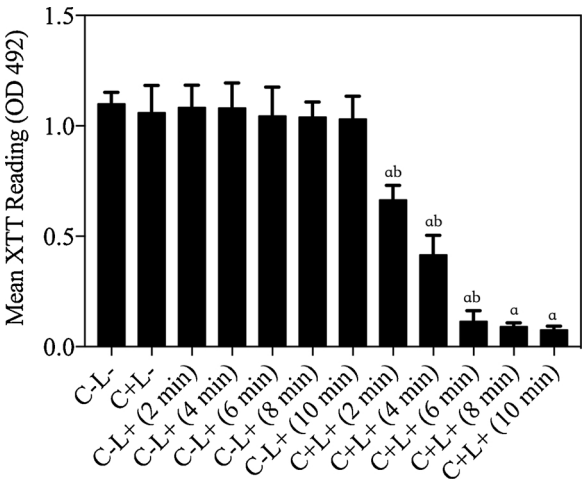

Fig. 4. Graphic representation of mean values and standard deviation of cell viabilities in ATCC 90028 *Candida albicans* biofilm under different illumination time.
[a], significant difference compared to control group (C-L-); [b], significant difference compared to the former group.

absorbance values obtained were statistically evaluated using one-way analysis of variance, and followed by the Tukey test for multiple comparisons (SPSS software, IBM®SPSS® Statistics, version 23). The $2^{-\Delta\Delta Ct}$ method was used to analyze the relative changes in gene expressions in the qRT-PCR experiments using Graph Pad Prism 6 Program (GraphPad Software, Inc., CA, USA), *t*-test Statistical significance was accepted for $p < 0.05$.

3. Results

3.1. Formation of C. albicans biofilms

The formation of *C. albicans* biofilms was visualized under inverted microscopy. The morphology variation from yeast buds microcolonies (2 h), pseudohypha and hyphae (12 h), to filamentous cells (24 h) and a dense mixture of yeasts, hyphae and matrix material in mature biofilms (48 h) were observed (Fig.1).

The metabolic activity of biofilms was demonstrated by XTT reduction assay. We found the readings of XTT increased with time and

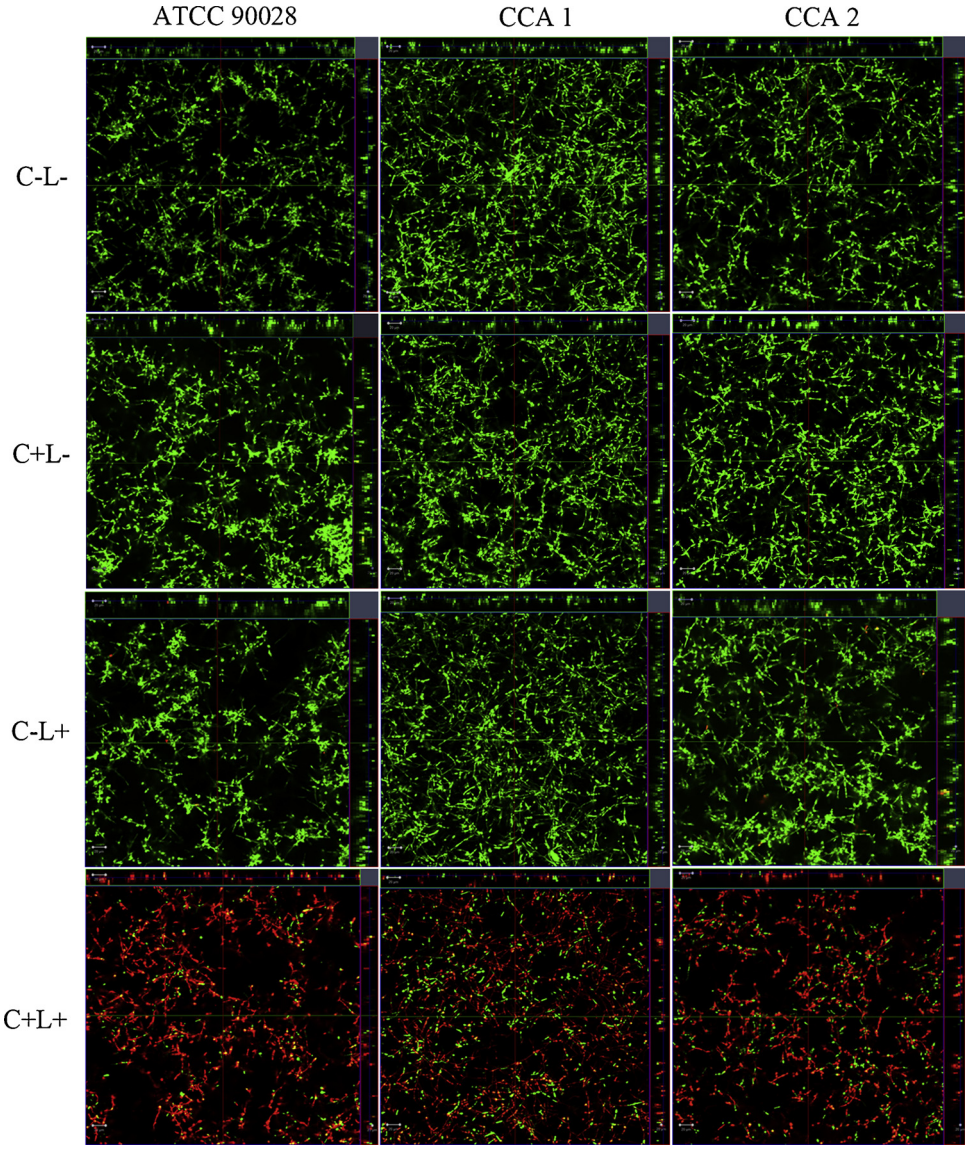

Fig. 5. Confocal laser scanning microscopy images of three specimens of *Candida albicans* biofilms under different conditions of CUR-PDT. Control group (C-L-) showed the biofilms treated without CUR or light. C + L- group showed the biofilms treated with curcumin alone. C-L + group showed the biofilms treated with light alone. C + L + group showed the biofilms treated with both curcumin (60 μM) and 6 min illumination.

they all reached a peak value at 48 h. (Fig.2).

3.2. Determination of optical parameters in CUR-PDT

The XTT mean values of ATCC 90028 *C. albicans* biofilms after exposure to the tested experimental conditions were presented in Fig.3 and Fig.4.

CUR-PDT using tested CUR concentrations (20, 40, 60, 80 and 100 μM) all showed an obvious reduction of biofilm viability in comparison to other groups. Under the same illumination period (4 min), the viabilities of biofilms were in a CUR concentration-dependent manner. XTT readings exhibited an inverse proportion with the CUR concentrations. According to the statistical results, 60 μM was chosen as an optimal CUR concentration for the following experiments.

Furthermore, CUR-PDT under tested illumination time (2, 4, 6, 8 and 10 min) all showed an obvious reduction of biofilm viability in comparison to other groups. Under the same CUR concentration (60 μM), the viabilities of biofilms showed an illumination time-dependent manner. XTT values decreased with the illumination time added. Among the five CUR-PDT groups, 6 min illumination time group was not statistically significant when compared with former groups ($p > 0.05$). Therefore, illumination time of 6 min was selected. Parameters in the clinical isolates groups were designated correspondingly.

3.3. Visualization and quantification of photodynamically treated C. albicans biofilms

Under the observation of CLSM, SYTO 9 penetrated all yeast membranes and stained them green. In contrast, PI only penetrated yeasts with damaged membranes, displacing SYTO 9 and stained them red. The images obtained by CLSM showed that after CUR-PDT, there was a distinguished increase in the number of cells marked with red fluorescence in all specimens of mature *C. albicans* biofilms, indicating fungal cell damage. Among them, CCA1 displayed the least red fluorescence, indicating the poorest inhibitory effect of CUR-PDT. In contrast, the fluorescence of red cells was hard to find in other groups (Fig.5).

It was also observed on CLSM images that the cells located on the superficial layers of the biofilm presented a bright intense fluorescence,

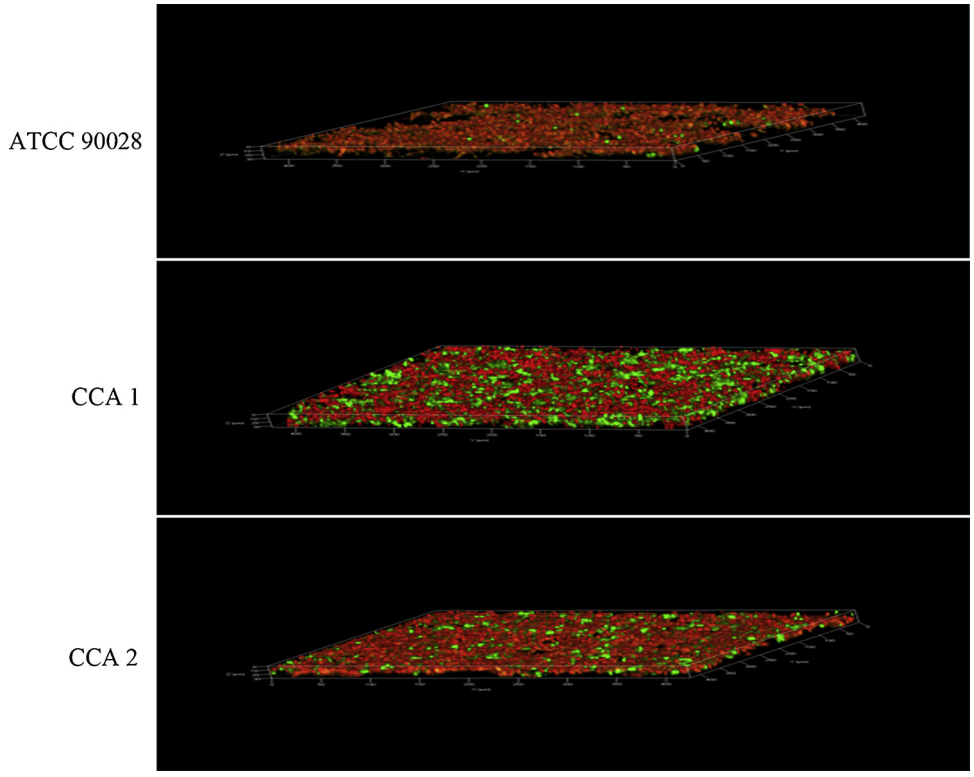

Fig. 6. 3D images of three specimens of *Candida albicans biofilms* after CUR-PDT.

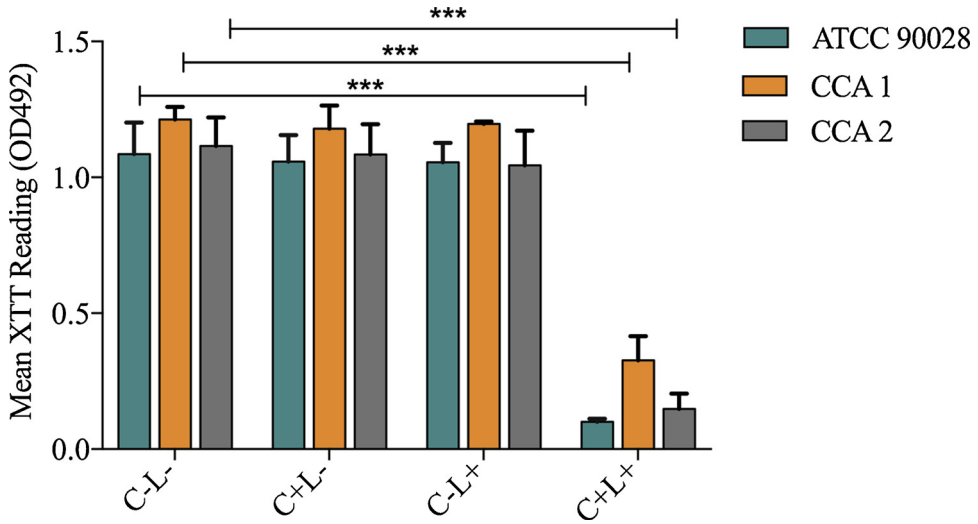

Fig. 7. Metabolic activity of *C. albicans* biofilms after CUR-PDT using 60 u M curcumin under 6 min illumination. The given values were the absorbance mean (XTT) ± standard deviation.
*, $p < 0.05$; **, $p < 0.01$; ***, $p < 0.001$.

Table 1
Metabolic activity of *Candida albicans* biofilms and the inhibition rate of three specimens after CUR-PDT.

	XTT ± SD	% of inhibition rate
ATCC C-L-	1.084 ± 0.067	NA
CCA1 C-L-	1.214 ± 0.026	NA
CCA2 C-L-	1.100 ± 0.030	NA
ATCC-PDT	0.099 ± 0.006	90.87
CCA1-PDT	0.386 ± 0.076	66.44
CCA2-PDT	0.148 ± 0.032	86.74

NA = not applicable; PDT = photodynamic therapy; C = Curcumin; L = LED light.

while in the basal layer the fluorescence was less intense or not present. This phenomenon was most obvious in CCA1 group (Fig.6).

To further quantify the inhibitory effect of CUR-PDT on *C. albicans* biofilms, we calculated the XTT values of all specimens using the optical parameters (CUR concentration 60 u M, illumination time 6 min) (Fig.7). We observed a significant decrease in the cell viability of CUR-PDT groups when compared with other groups. Based on the same experimental conditions in this study, CCA1 and CCA2 appeared to be more virulent than the standard strain. Both XTT values and inhibition rates in CCA1 and CCA2 were lower than the standard strain group (Table 1).

Transcriptional levels of hypha-specific and biofilm-related genes

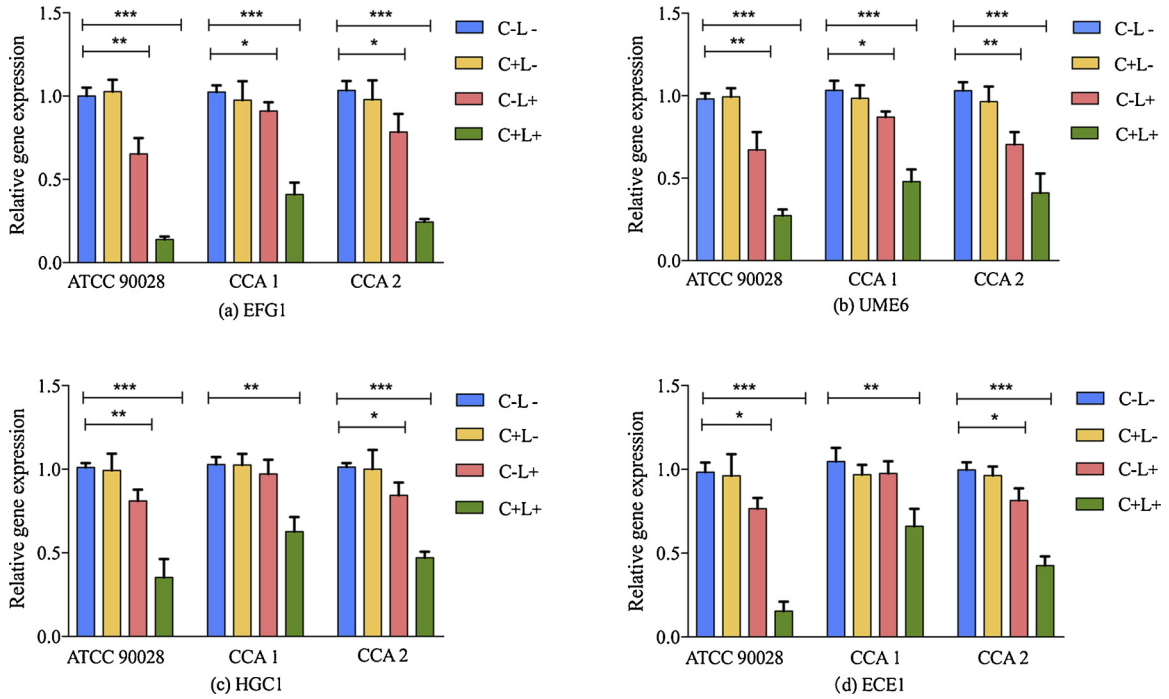

Fig. 8. Relative genes expression of EFG1 (Fig. 8a), UME6 (Fig. 8b), HGC1 (Fig. 8c), and ECE1 (Fig. 8d) in control group (C-L-) by quantitative real-time PCR (qRT-PCR) in relation to the groups C + L-, C-L+, and C + L+ using CUR-PDT. Values were expressed as the mean ± standard deviation.
*, $p < 0.05$; **, $p < 0.01$; ***, $p < 0.001$.

Table 2
Fold-decrease and p values for the genes EFG1, UME6, HGC1, and ECE1 after treatment with CUR-PDT.

	ATCC 90028 Fold-decrease, p values	CCA1 Fold-decrease, p values	CCA2 Fold-decrease, p values
EFG1	6.865, $p < 0.0001$	2.466, $p = 0.0002$	5.406, $p < 0.0001$
UME6	3.382, $p < 0.0001$	2.146, $p = 0.0021$	2.347, $p = 0.0005$
HGC1	2.167, $p < 0.0001$	1.627, $p = 0.0021$	2.073, $p = 0.0005$
ECE1	6.887, $p < 0.0001$	3.102, $p = 0.0070$	3.711, $p = 0.0020$

EFG1, UME6, HGC1 and ECE1 were quantified by qRT-PCR. All analyzed genes were downregulated after CUR-PDT (C + L+). Group C + L- did not demonstrate down or upregulation when compared with the control group C-L-. However, genes were also downregulated in group C-L+, indicating that light alone can destruct the biofilm formation to a certain extent (Fig.8). The fold changes of CUR-PDT groups compared with control group were illustrated in Table 2.

4. Discussion

C. albicans is the predominant pathogen among all fungal species which can cause more than 50% of clinical cases including local and invasive candidiasis [26–28]. Oral candidiasis remains the most commonly encountered oral manifestation in HIV patients [29]. OLP, a chronic inflammatory oral mucosal disorder, is also frequently associated with oral Candidal infection [30,31]. Studies have shown biofilm-associated Candidal infections in HIV and OLP patients are even more refractory as their sessile living cells show high resistance to antifungal treatment and host defense mechanisms [32,33].

In recent years, PDT has emerged as a promising strategy to eliminate *C. albicans* biofilms [10,34,35]. Studies have revealed that the combination of CUR with blue LED light was also effective in the antifungal activity against both planktonic [24] and biofilm form of the yeasts [25,36,37]. These results demonstrated that CUR might be a desirable photosensitizer for PDT against *C. albicans* infections.

Therefore, we evaluated the inhibitory effects of CUR-PDT against biofilms of one standard strain and two clinical isolates of *C.albicans* obtained from HIV-infected patient and OLP patient.

Our inhibition rate of *C. albicans* biofilms after CUR-PDT in ATCC 90028 strain (90.87%) differed from the result from Dovigo et al. (87.22%) [25]. In clinical isolates groups, inhibition rates were much lower (66.44% in CCA1, 86.74% in CCA2) when compared with standard one, and this result was in accordance with other researchers' findings [24,38–40]. One possible explanation is the different virulence of each strain, as clinical isolates tend to be more virulent than standard one, which may vary according to the isolate itself and the internal environment of the host.

CLSM observations indicated the significant antifungal effect of CUR-PDT on *C. albicans* biofilms. Obvious increase of red fluorescent cells after CUR-PDT were observed, suggesting extensive cell photodamage. Interestingly, the different brightness among the layers of the biofilms was also observed. The outermost layer exhibited brighter fluorescence than basal layer. This phenomenon was in accordance with the study of Andrade et al. and Pereira et al [41,42]. These may be caused by the defining characteristic extracellular matrix (ECM) of fungal biofilms. ECM might function to serve as a scaffold for maintaining biofilm integrity and to limit diffusion of toxic substances into the biofilm [43]. The complexity and tightness in structure protected the basal cells from photosensitizer penetration and inactivation of PDT which has been verified in light microscopy observation in our study as well. These results may explain why CUR-PDT is not able to eliminate all the cells in *C. albicans* biofilms in the present study.

It is worth to note that former researchers mainly focused on the variations of dosimetry in PDT and its correlation with their antifungal effectiveness. However, in this study, gene expressions related to *C. albicans* biofilms formation were also taken into investigation for the first time. We believe these results would further reveal the alterations in biofilms when treated with PDT from a new perspective.

In the present study, the transcriptional levels of several hypha-specific and biofilm-related genes were significantly altered by CUR-PDT both at the hyphal initiation (EFG1) stage and long-term

maintenance (UME6, HGC1, and ECE1) stage [44–46]. Expressions of these four genes were all downregulated in three specimens, indicating CUR-PDT destructed hyphal growth, induced cell separation and therefore impaired biofilm formation. EFG1 positively regulates the formation of hyphae in initial *C. albicans* biofilms [47,48]. In a PDT study using MB as a photosensitizer, Freire et al. [49] also found that EFG1 was downregualted in PDT-treated *C. albicans* biofilms, resulting initial hyphal reduction. On the other hand, *C. albicans* filamentation requires cell polarized growth as well as long-time maintenance of cell separation, during which UME6, HGC1 and ECE1 are activated [50–52]. These genes are essential for hyphal development and their expressions have been shown to be correlated with cell elongation and biofilm formation [53,54]. Our data suggested that CUR-PDT may inhibit hyphae and biofilm formation by downregulating these hypha-specific and biofilm-related genes.

Interestingly, these genes were also downregulated in light alone group (C-L+), indicating that light itself can influence the hyphae formation. We suppose it may be relevant to the phototoxicity of DNA in the process of PDT. Studies have reported that the wavelength used in the present study (455 nm) may cause oxidative stress by accumulation of reactive oxygen species (ROS) which may induce minute DNA damage in cells [55,56]. However its antifungal effect was not comparable to the photoinactivation of PDT. This phenomenon reminded us to be cautious of the phototoxicity of PDT and the protection of adjacent tissue when used in clinic.

In conclusion, our results may contribute a little more to the advancement of PDT, however, within the limitation of our study, there are still some aspects that remain to be better elucidated. Further *in vivo* investigations should be carried out in the future.

Declaration of Competing Interest

Jing Ma and Hang Shi contributed equally to the work so they should be considered as co-first authors.

Acknowledgements

The present study was supported by Medical Guiding Project, Science and Technology Commission of Shanghai Municipality, China (Grant No. 134119a8700).

References

[1] T. Ohshima, S. Ikawa, K. Kitano, N. Maeda, A proposal of remedies for oral diseases caused by *Candida*: a mini review, Front. Microbiol. 9 (2018) 1522.
[2] D.R. Marable, L.M. Bowers, T.L. Stout, et al., Oral candidiasis following steroid therapy for oral lichen planus, Oral Dis. 22 (2) (2016) 140–147.
[3] A. Amer, S. Galvin, C.M. Healy, G.P. Moran, The microbiome of potentially malignant oral leukoplakia exhibits enrichment for Fusobacterium, Leptotrichia, Campylobacter, and Rothia species, Front. Microbiol. 8 (2017) 2391.
[4] C. Medeiros, L.G. Dos Anjos Borges, K. Cherubini, F.G. Salum, Medina da Silva R, de Figueiredo M. Oral yeast colonization in patients with primary and secondary Sjögren's syndrome, Oral Dis. 24 (7) (2018) 1367–1378.
[5] M. Mohd Bakri, H. Mohd Hussaini, A. Rachel Holmes, R. David Cannon, A. Mary Rich, Revisiting the association between candidal infection and carcinoma, particularly oral squamous cell carcinoma, J. Oral Microbiol. (2010) 2.
[6] S. Tulasidas, P. Rao, S. Bhat, R. Manipura, A study on biofilm production and antifungal drug resistance among *Candida* species from vulvovaginal and bloodstream infections, Infect. Drug Resist. 11 (2018) 2443–2448.
[7] G. Ramage, K. Vande Walle, B.L. Wickes, J.L. López-Ribot, Standardized method for in vitro antifungal susceptibility testing of *Candida albicans* biofilms, Antimicrob. Agents Chemother. 45 (9) (2001) 2475–2479.
[8] J. Chandra, P.K. Mukherjee, S.D. Leidich, et al., Antifungal resistance of candidal biofilms formed on denture acrylic in vitro, J. Dent. Res. 80 (3) (2001) 903–908.
[9] S. Dong, H. Shi, X. Zhang, et al., Difunctional bacteriophage conjugated with photosensitizers for *Candida albicans*-targeting photodynamic inactivation, Int. J. Nanomedicine 13 (2018) 2199–2216.
[10] H. Shi, J. Li, H. Zhang, J. Zhang, H. Sun, Effect of 5-aminolevulinic acid photodynamic therapy on *Candida albicans* biofilms: an in vitro study, Photodiagnosis Photodyn. Ther. 15 (2016) 40–45.
[11] T.J. Dougherty, C.J. Gomer, B.W. Henderson, et al., Photodynamic therapy, J. Natl. Cancer Inst. 90 (12) (1998) 889–905.
[12] R.R. Allison, G.H. Downie, R. Cuenca, X.H. Hu, C.J. Childs, C.H. Sibata, Photosensitizers in clinical PDT, Photodiagnosis Photodyn. Ther. 1 (1) (2004) 27–42.
[13] A.P. Pinto, I.B. Rosseti, M.L. Carvalho, B. da Silva, C. Alberto-Silva, M.S. Costa, Photodynamic Antimicrobial Chemotherapy (PACT), using Toluidine blue O inhibits the viability of biofilm produced by *Candida albicans* at different stages of development, Photodiagnosis Photodyn. Ther. 21 (2018) 182–189.
[14] E.J. Prażmo, M. Kwaśny, M. Łapiński, A. Mielczarek, Photodynamic therapy As a promising method used in the treatment of oral diseases, Adv. Clin. Exp. Med. 25 (4) (2016) 799–807.
[15] G.A. da Collina, F. Freire, T. Santos, et al., Controlling methylene blue aggregation: a more efficient alternative to treat *Candida albicans* infections using photodynamic therapy, Photochem. Photobiol. Sci. 17 (10) (2018) 1355–1364.
[16] A. Azizi, Z. Amirzadeh, M. Rezai, S. Lawaf, A. Rahimi, Effect of photodynamic therapy with two photosensitizers on Candida albicans, J. Photochem. Photobiol. B 158 (2016) 267–273.
[17] M.C. Huang, M. Shen, Y.J. Huang, H.C. Lin, C.T. Chen, Photodynamic inactivation potentiates the susceptibility of antifungal agents against the planktonic and biofilm cells of Candida albicans, Int. J. Mol. Sci. 19 (2) (2018).
[18] M.L. Lestari, G. Indrayanto, Curcumin, Profiles Drug Subst. Excip. Relat. Methodol. 39 (2014) 113–204.
[19] K. Park, J.H. Lee, Photosensitizer effect of curcumin on UVB-irradiated HaCaT cells through activation of caspase pathways, Oncol. Rep. 17 (3) (2007) 537–540.
[20] R. Mohan, J. Sivak, P. Ashton, et al., Curcuminoids inhibit the angiogenic response stimulated by fibroblast growth factor-2, including expression of matrix metalloproteinase gelatinase B, J. Biol. Chem. 275 (14) (2000) 10405–10412.
[21] B.B. Aggarwal, A. Kumar, A.C. Bharti, Anticancer potential of curcumin: preclinical and clinical studies, Anticancer Res. 23 (1A) (2003) 363–398.
[22] S.Z. Moghadamtousi, H.A. Kadir, P. Hassandarvish, H. Tajik, S. Abubakar, K. Zandi, A review on antibacterial, antiviral, and antifungal activity of curcumin, Biomed Res. Int. (2014) 186864.
[23] S. Ghosh, S. Banerjee, P.C. Sil, The beneficial role of curcumin on inflammation, diabetes and neurodegenerative disease: a recent update, Food Chem. Toxicol. 83 (2015) 111–124.
[24] L.N. Dovigo, A.C. Pavarina, J.C. Carmello, A.L. Machado, I.L. Brunetti, V.S. Bagnato, Susceptibility of clinical isolates of *Candida* to photodynamic effects of curcumin, Lasers Surg. Med. 43 (9) (2011) 927–934.
[25] L.N. Dovigo, A.C. Pavarina, A.P. Ribeiro, et al., Investigation of the photodynamic effects of curcumin against Candida albicans, Photochem. Photobiol. 87 (4) (2011) 895–903.
[26] D.S. Perlin, R. Rautemaa-Richardson, A. Alastruey-Izquierdo, The global problem of antifungal resistance: prevalence, mechanisms, and management, Lancet Infect. Dis. 17 (12) (2017) e383–e392.
[27] A.L. Colombo, J. Perfect, M. DiNubile, et al., Global distribution and outcomes for *Candida* species causing invasive candidiasis: results from an international randomized double-blind study of caspofungin versus amphotericin B for the treatment of invasive candidiasis, Eur. J. Clin. Microbiol. Infect. Dis. 22 (8) (2003) 470–474.
[28] M.A. de Resende, L.V. de Sousa, R.C. de Oliveira, C.Y. Koga-Ito, J.P. Lyon, Prevalence and antifungal susceptibility of yeasts obtained from the oral cavity of elderly individuals, Mycopathologia. 162 (1) (2006) 39–44.
[29] A. El Howati, A. Tappuni, Systematic review of the changing pattern of the oral manifestations of HIV, J. Investig. Clin. Dent. 9 (4) (2018) e12351.
[30] G.P. Bombeccari, A.B. Giannì, F. Spadari, Oral *Candida* colonization and oral lichen planus, Oral Dis. 23 (7) (2017) 1009–1010.
[31] M. Hertel, A.M. Schmidt-Westhausen, F.P. Strietzel, Local, systemic, demographic, and health-related factors influencing pathogenic yeast spectrum and antifungal drug administration frequency in oral candidiasis: a retrospective study, Clin. Oral Investig. 20 (7) (2016) 1477–1486.
[32] J.V. Desai, A.P. Mitchell, D.R. Andes, Fungal biofilms, drug resistance, and recurrent infection, Cold Spring Harb. Perspect. Med. 4 (10) (2014).
[33] J. Chandra, D.M. Kuhn, P.K. Mukherjee, L.L. Hoyer, T. McCormick, M.A. Ghannoum, Biofilm formation by the fungal pathogen *Candida albicans*: development, architecture, and drug resistance, J. Bacteriol. 183 (18) (2001) 5385–5394.
[34] M.P. Silva, T.A. dos Santos, P.P. de Barros, F. de Camargo Ribeiro, J.C. Junqueira, A.O. Jorge, Action of antimicrobial photodynamic therapy on heterotypic biofilm: *candida albicans* and Bacillus atrophaeus, Lasers Med. Sci. 31 (4) (2016) 605–610.
[35] S. Khan, F. Alam, A. Azam, A.U. Khan, Gold nanoparticles enhance methylene blue-induced photodynamic therapy: a novel therapeutic approach to inhibit *Candida albicans* biofilm, Int. J. Nanomedicine 7 (2012) 3245–3257.
[36] V.T. Sakima, P.A. Barbugli, P.S. Cerri, et al., Antimicrobial photodynamic therapy mediated by curcumin-loaded polymeric nanoparticles in a murine model of oral candidiasis, Molecules. 23 (8) (2018).
[37] L.N. Dovigo, J.C. Carmello, C.A. de Souza Costa, et al., Curcumin-mediated photodynamic inactivation of *Candida albicans* in a murine model of oral candidiasis, Med. Mycol. 51 (3) (2013) 243–251.
[38] L.N. Dovigo, A.C. Pavarina, E.G. Mima, E.T. Giampaolo, C.E. Vergani, V.S. Bagnato, Fungicidal effect of photodynamic therapy against fluconazole-resistant *Candida albicans* and *Candida glabrata*, Mycoses. 54 (2) (2011) 123–130.
[39] A.S. Garcia-Gomes, J.A. Curvelo, R.M. Soares, A. Ferreira-Pereira, Curcumin acts synergistically with fluconazole to sensitize a clinical isolate of *Candida albicans* showing a MDR phenotype, Med. Mycol. 50 (1) (2012) 26–32.
[40] S.A. Lambrechts, M.C. Aalders, F.D. Verbraak, J.W. Lagerberg, J.B. Dankert, J.J. Schuitmaker, Effect of albumin on the photodynamic inactivation of microorganisms by a cationic porphyrin, J. Photochem. Photobiol. B 79 (1) (2005) 51–57.
[41] C.A. Pereira, R.L. Romeiro, A.C. Costa, A.K. Machado, J.C. Junqueira, A.O. Jorge,

Susceptibility of *Candida albicans*, Staphylococcus aureus, and Streptococcus mutans biofilms to photodynamic inactivation: an in vitro study, Lasers Med. Sci. 26 (3) (2011) 341–348.
[42] M.C. Andrade, A.P. Ribeiro, L.N. Dovigo, et al., Effect of different pre-irradiation times on curcumin-mediated photodynamic therapy against planktonic cultures and biofilms of *Candida* spp, Arch. Oral Biol. 58 (2) (2013) 200–210.
[43] J.R. Blankenship, A.P. Mitchell, How to build a biofilm: a fungal perspective, Curr. Opin. Microbiol. 9 (6) (2006) 588–594.
[44] Y. Li, Y. Ma, L. Zhang, et al., In vivo inhibitory effect on the biofilm formation of *Candida albicans* by liverwort derived riccardin D, PLoS One 7 (4) (2012) e35543.
[45] J.C. Marioni, C.E. Mason, S.M. Mane, M. Stephens, Y. Gilad, RNA-seq: an assessment of technical reproducibility and comparison with gene expression arrays, Genome Res. 18 (9) (2008) 1509–1517.
[46] A.B. Parsons, A. Lopez, I.E. Givoni, et al., Exploring the mode-of-action of bioactive compounds by chemical-genetic profiling in yeast, Cell. 126 (3) (2006) 611–625.
[47] T. Lassak, E. Schneider, M. Bussmann, et al., Target specificity of the *Candida albicans* Efg1 regulator, Mol. Microbiol. 82 (3) (2011) 602–618.
[48] G. Ramage, K. VandeWalle, J.L. López-Ribot, B.L. Wickes, The filamentation pathway controlled by the Efg1 regulator protein is required for normal biofilm formation and development in Candida albicans, FEMS Microbiol. Lett. 214 (1) (2002) 95–100.
[49] F. Freire, P.P. de Barros, C.A. Pereira, J.C. Junqueira, A. Jorge, Photodynamic inactivation in the expression of the *Candida albicans* genes ALS3, HWP1, BCR1, TEC1, CPH1, and EFG1 in biofilms, Lasers Med. Sci. 33 (7) (2018) 1447–1454.
[50] H. Liu, Transcriptional control of dimorphism in Candida albicans, Curr. Opin. Microbiol. 4 (6) (2001) 728–735.
[51] P.L. Carlisle, M. Banerjee, A. Lazzell, C. Monteagudo, J.L. López-Ribot, D. Kadosh, Expression levels of a filament-specific transcriptional regulator are sufficient to determine *Candida albicans* morphology and virulence, Proc Natl Acad Sci U S A. 106 (2) (2009) 599–604.
[52] R.H. Liu, Z.C. Shang, T.X. Li, M.H. Yang, L.Y. Kong, In vitro antibiofilm activity of eucarobustol e against Candida albicans, Antimicrob. Agents Chemother. 61 (8) (2017).
[53] C.J. Nobile, D.R. Andes, J.E. Nett, et al., Critical role of Bcr1-dependent adhesins in *C. albicans* biofilm formation in vitro and in vivo, PLoS Pathog. 2 (7) (2006) e63.
[54] D. Wilson, J.R. Naglik, B. Hube, The missing link between *Candida albicans* hyphal morphogenesis and host cell damage, PLoS Pathog. 12 (10) (2016) e1005867.
[55] M. Maclean, S.J. Macgregor, J.G. Anderson, G.A. Woolsey, The role of oxygen in the visible-light inactivation of Staphylococcus aureus, J. Photochem. Photobiol. B 92 (3) (2008) 180–184.
[56] M.R. Hamblin, J. Viveiros, C. Yang, A. Ahmadi, R.A. Ganz, M.J. Tolkoff, Helicobacter pylori accumulates photoactive porphyrins and is killed by visible light, Antimicrob. Agents Chemother. 49 (7) (2005) 2822–2827.